

STREAMS: An Assistive Multimodal AI Framework for Empowering Biosignal Based Robotic Controls

Ali Rabiee¹, Sima Ghafoori¹, Xiangyu Bai², Sarah Ostadabbas², Reza Abiri¹

Abstract—End-effector based assistive robots face persistent challenges in generating smooth and robust trajectories when controlled by human’s noisy and unreliable biosignals such as muscle activities and brainwaves. The produced endpoint trajectories are often jerky and imprecise to perform complex tasks such as stable robotic grasping. We propose STREAMS (Self-Training Robotic End-to-end Adaptive Multimodal Shared autonomy) as a novel framework leveraged deep reinforcement learning to tackle this challenge in biosignal based robotic control systems. STREAMS blends environmental information and synthetic user input into a Deep Q Learning Network (DQN) pipeline for an interactive end-to-end and self-training mechanism to produce smooth trajectories for the control of end-effector based robots. The proposed framework achieved a high-performance record of 98% in simulation with dynamic target estimation and acquisition without any pre-existing datasets. As a zero-shot sim-to-real user study with five participants controlling a physical robotic arm with noisy head movements, STREAMS (as an assistive mode) demonstrated significant improvements in trajectory stabilization, user satisfaction, and task performance reported as a success rate of 83% compared to manual mode which was 44% without any task support. STREAMS seeks to improve biosignal based assistive robotic controls by offering an interactive, end-to-end solution that stabilizes end-effector trajectories, enhancing task performance and accuracy.

I. INTRODUCTION

Assistive technologies aim to restore independence for individuals with severe motor impairments by providing various control interfaces, including non-invasive options like head arrays [1], body-machine interfaces [2], [3], eye-tracking systems [4], [5], electroencephalogram (EEG) [6]–[8], and electromyography (EMG) muscle activity [9], as well as invasive solutions such as cortical implants [10].

However, such individualized biosignal based control approaches and their associated decoders are not able to generate stable outputs (trajectories) particularly when facing the challenge of continuous control of an end-effector based system (e.g. computer cursor) for accurate target acquisition (Fig 1) [11], [12]. This challenge could be more destructive when controlling the endpoint of a physical robotic system

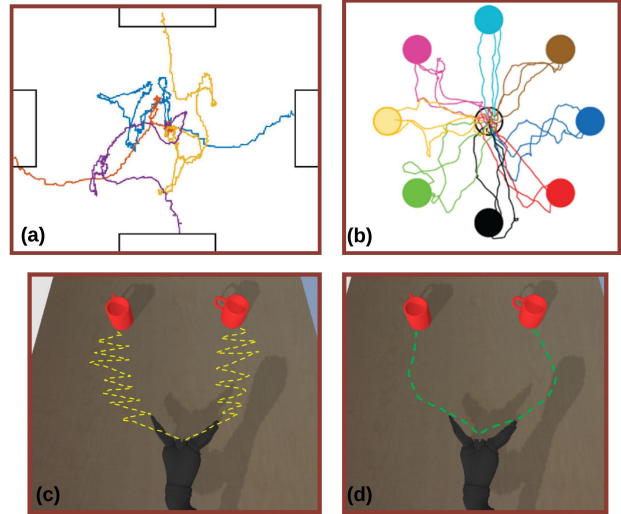


Fig. 1: Example of traveled trajectories by the end-effector based systems. (a) EEG-based [11] and (b) Electrocorticography (ECoG)-based brain computer interface (BCI) studies [12] for computer cursor control tasks (adopted from our previous studies). The projection of such generated jerky trajectories in controlling the endpoint of robotic arms showed low performance in success rate [13]. (c) Conceptual representation of robotic arm trajectories with jerky and unreliable human input. (d) Conceptual representation of stable robotic arm trajectories modified by assistive algorithms such as STREAMS, demonstrating smoother paths to targets.

where a minimum jerky motion causes failure in tasks such as robotic grasping for a patient with severe motor impairment [14]. Additionally, the required high level of engagement for continuous control of traveled trajectory imposes a high cognitive load on most patients particularly those with brain implants [12]. This cognitive burden was further escalated by the uncertainty of human intention decoders in real-world scenarios of human-robot collaboration for target acquisition, as studied by Dani et al. [15]. Most of the previous research studies on shared human-robot control [16]–[19] assumed known or explicitly predicted targets, lacking real-time responsiveness to dynamic user intentions, demands, or changes in the environment’s structure. To this end, we present STREAMS (Self-Training Robotic End-to-end Adaptive Multimodal Shared autonomy), a novel framework using deep reinforcement learning along with a DQN approach, to overcome the barriers of current human-robot shared control approaches in reach-to-grasp objects in 2D workspace by focusing on the following highlighted

*This work was supported by RI-INBRE (NIH P20GM103430) & NSF award ID 2245558.

**Code: <https://github.com/ali-rabiee/STREAMS>

¹Ali Rabiee, Sima Ghafoori, and Reza Abiri (corresponding author) are with the Department of Electrical Engineering, University of Rhode Island, Kingston, RI, USA, 02881. emails: {ali.rabiee, sima.ghafoori, reza.abiri}@uri.edu

²Sarah Ostadabbas and Xiangyu Bai are with the Department of Electrical and Computer Engineering, Northeastern University, 360 Huntington Avenue, Boston, Massachusetts, USA, 02115 emails: ostadabbas@ece.neu.edu, bai.xiang@northeastern.edu

contributions:

- Proposed an adaptive trajectory generation method using deep reinforcement learning to produce smooth, reliable paths in complex, dynamic environments, even under noisy and imprecise biosignal control inputs.
- Developed an interactive end-to-end multimodal framework that directly translates unreliable biosignal inputs and environmental perception into appropriate robotic actions. This approach eliminates the need for intermediate representations or explicit intention recognition.
- Designed a self-training DQN-based framework that eliminates the need for any datasets by leveraging synthetic data that emulates real-world biosignal noise.
- Demonstrated a zero-shot sim-to-real translation of our framework and validated the generalizability and adaptivity of our pipeline for practical cases through a user study.

II. RELATED WORK

Shared autonomy paradigms in end-effector based assistive robots have explored different approaches such as sequential, arbitrated, and learning policies to balance user control and robotic assistance. Jain et al. [20] introduced a shared control paradigm blending user inputs with the perception of the environment through sequential policies. However, their system demanded significant user input and imposed a high cognitive load. Additionally, it relied on pre-programmed actions, limiting its adaptability to new conditions and diverse objects. Downey et al. [21] developed a shared control paradigm that arbitrated between a neural spikes decoder and autonomous robotic assistance for object manipulation. Their approach was constrained by pre-defined rules without interactivity with users, making it unable to dynamically adapt to user inputs or evolving situations. Muelling et al. [22] developed a continuous assistance method using arbitrated policies based on a probability distribution over goals but was not able to address the challenge of handling imprecise user inputs and varied intents. Xu et al. [23] reported a shared control paradigm that arbitrated between an EEG-based brain-computer interface (BCI) and computer vision guidance based on the robotic arm’s endpoint location relative to the target. However, it was tested only with fixed or randomly placed single targets and did not address more complex scenarios or multi-object environments. Beraldo et al. [24] presented a shared autonomy paradigm that fused user input and environmental context by relying on a set of predefined policies to predict the next subgoal for a navigation task. While effective for navigation, the system’s ability to generalize to more complex tasks, such as reach-to-grasp, was not evaluated. Additionally, the reliance on predefined policies restricts the adaptability of the system to dynamically changing environments and user preferences. Furthermore, A key limitation of most methods for end-effector based robots is their dependency on user datasets for training, explicit goal prediction, and predefined policies. In contrast, our work presented an end-to-end self-training approach that delivers continuous and interactive assistance

in dynamic multi-target environments in which the user intention may be ambiguous without depending on datasets. It could be adaptable to a wide range of scenarios and prioritizes stabilizing endpoint trajectories, enabling precise robotic grasping in assistive robotics.

III. METHODS

A. Problem formulation and framework

We propose STREAMS framework based on Deep Q-Networks (DQN) for the control problem defined as a Partially Observable Markov Decision Process (POMDP). The main goal of our framework is to enable the end-effector to reach and grasp the intended object following a smooth trajectory based on environmental perception even with imprecise human input. As illustrated in Fig. 2, the STREAMS framework captures and preprocesses the environment image, and analyzes it with user input coming from the potential control interface to determine optimal robotic arm actions using a Deep Q-Network. After executing the chosen action, the resulting new state of the environment is fed back into the system, creating an adaptive control loop.

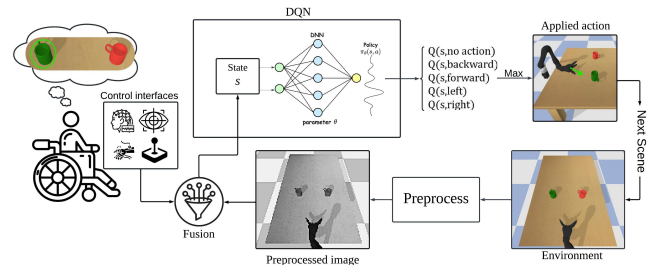


Fig. 2: Pipeline of the STREAMS framework for adaptive control of an assistive robotic arm using multimodal inputs coming from potential control interfaces and environment perception.

Let \mathcal{S} denote the state space, which is composed of two key components: environment perception and human input. Assuming a severely impaired user (tetraplegia), we used head movement input with injected noise to simulate the imprecision typically seen in biosignal decoders. The environment perception is captured through a sequence of 2D grayscale images $I_t \in \mathbb{R}^{H \times W}$, while the unreliable and imprecise human control input is represented as \tilde{h}_t . The state s_t at time t is defined as the concatenation of the last N frames:

$$s_t = \{I_{t-N+1}, \dots, I_t, \tilde{h}_{t-N+1}, \dots, \tilde{h}_t\} \quad (1)$$

In our case study, we consider $\tilde{h}_t \in \{-1, 0, 1\}$, which represents decoded values of 1D head movements corresponding to left, neutral, and right, respectively. The action space \mathcal{A} consists of five possible actions: forward, backward, right, left, and hold. We focus on controlling the end-effector position directly, while the positions of other joints in the robotic arm are determined using inverse kinematics. The Q-value function $Q(s_t, a)$ is approximated by a DQN, which

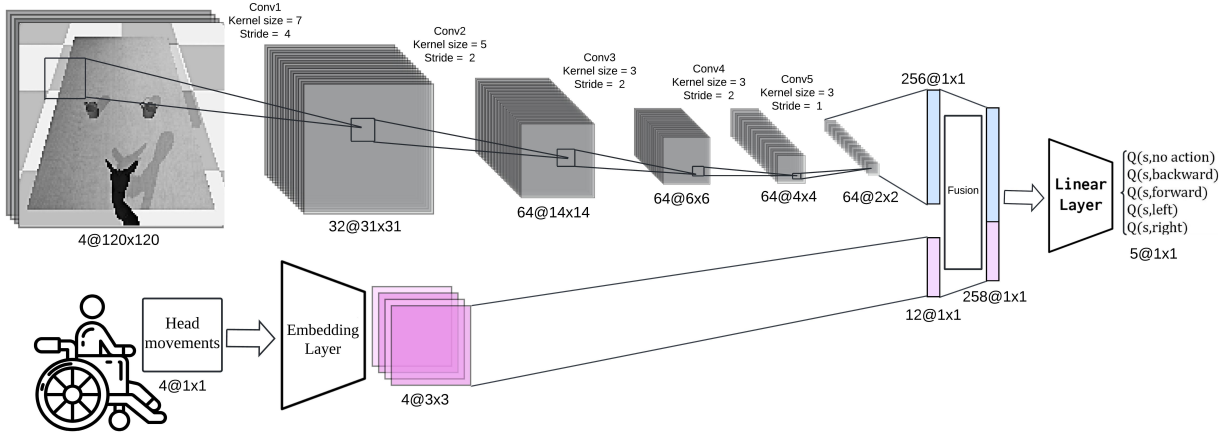


Fig. 3: The STREAMS framework’s Deep Q-Network architecture processes stacked grayscale images and user inputs from the last four timesteps. Grayscale inputs pass through five convolutional layers, while user inputs are handled via an embedding layer, with both fused to output Q-values for five possible actions.

integrates convolutional layers to process image inputs, embedding layers to represent human inputs, and a late fusion mechanism to combine information from both modalities. The output is passed through linear layers to make the final action decision as it illustrated in Fig 3.

We explore three distinct reward functions to guide the learning process:

1. Binary reward (R_1): A simple binary reward where success is defined by the end-effector reaching and grasping the target object.

$$R_1(s_t, a_t) = \begin{cases} 1, & \text{if success} \\ 0, & \text{otherwise} \end{cases} \quad (2)$$

2. Distance-based reward (R_2): This reward also incorporates the distance between the end-effector and the target object, rewarding the agent for reducing this distance.

$$R_2(s_t, a_t) = \begin{cases} 1, & \text{if success} \\ \alpha \cdot \left(1 - \frac{d_t}{d_{init}}\right), & \text{if episode is ongoing} \\ 0, & \text{otherwise} \end{cases} \quad (3)$$

3. Time-penalized distance-based reward (R_3): This reward is similar to the distance-based reward but includes a time penalty to encourage faster task completion.

$$R_3(s_t, a_t) = R_2(s_t, a_t) - \beta \cdot t, \quad (4)$$

In these functions, d_t is the distance between end-effector and the target at each time step, d_{init} is the initial distance at the beginning of each episode, and α and β are hyperparameters between 0 and 1. A threshold is set for the euclidean distance between the end-effector and the target. When this distance exceeds the threshold, a grasp action is automatically triggered. The episode then concludes with the grasping attempt being evaluated as either successful or

failed. Additionally, if the robot does not reach the target within 18 time steps, the episode is deemed a failure.

During training, a synthetic user is developed to simulate the unreliable nature of human control input by generating ideal inputs (h_t^{ideal}) and adding noise to them. The ideal inputs represent the optimal, precise control inputs that guide the end-effector to the target object. This noise is introduced by randomly flipping input values with a probability (p), creating noisy and inaccurate inputs (\tilde{h}_t). By adjusting the noise level, input uncertainty can be varied. This synthetic approach eliminates the need for datasets and human intervention, speeding up the training process and improving the framework’s ability to handle varying input quality. The input \tilde{h}_t is generated from the ideal input h_t^{ideal} as follows:

$$\tilde{h}_t = \begin{cases} h_t^{ideal}, & \text{with probability } 1 - p \\ \text{Flip}(h_t^{ideal}), & \text{with probability } p \end{cases} \quad (5)$$

Here, the function $\text{Flip}(h_t^{ideal})$ randomly changes h_t^{ideal} to one of the other two possible values $\{-1, 0, 1\}$. The noise generation process presented here for our head movement signal is oriented to the characteristics of EEG signals, which normally have a lower SNR compared with other biosignals [25]. Different studies [26]–[29] show that for the multiclass motor imagery classification problem using EEG, typical decoder accuracies range between 70% and 90%. The same variability in decoder outputs is emulated here by considering three different levels of noise assigned probabilities (p) of 0.2, 0.3, and 0.4 during the training phase. The pseudocode for the training phase of the algorithm is presented in Algorithm 1. The DQN in the STREAMS framework is trained using experience replay, where past experiences (s_t, a_t, r_t, s_{t+1}) are stored in a replay buffer, and mini-batches are sampled to update the network parameters θ . A target network with parameters θ' is used to stabilize learning. The loss function involves the difference between the predicted and target Q-values, incorporating the reward

r and discount factor γ . The performance is evaluated on metrics such as task success rate, trajectory efficiency, and robustness to input noise. STREAMS is trained in a simulated environment with a hyperparameter random search using the Adam optimizer and an ϵ -greedy strategy for exploration, with ϵ decaying from 0.9 to 0.1. Training includes 25,000 episodes and randomization of cup positions to prevent overfitting and enhance generalization across tasks.

Algorithm 1 DQN-Based Reach-to-Grasp Control with Synthetic Noise

```

Initialize replay buffer  $\mathcal{D}$ 
Initialize primary network  $Q(s, a; \theta)$  and target network  $Q'(s', a'; \theta')$  with random weights
for each episode do
  Initialize state  $s_1 = \{I_{1-N+1}, \dots, I_1, \tilde{h}_{1-N+1}, \dots, \tilde{h}_1\}$ 
  for each step  $t$  in episode do
    With probability  $\epsilon$ , select random action  $a_t$ 
    Otherwise, select  $a_t = \arg \max_a Q(s_t, a; \theta)$ 
    Execute action  $a_t$ 
    Observe reward  $r_t$  and next state  $s_{t+1}$ 
    Generate noisy human input  $\tilde{h}_t$ :
    if With probability  $1 - p$  then
      set  $\tilde{h}_t = h_t^{ideal}$ 
    else
      set  $\tilde{h}_t = \text{Flip}(h_t^{ideal})$ 
    end if
    Store transition  $(s_t, a_t, r_t, s_{t+1})$ 
    Sample mini-batch of transitions  $(s_j, a_j, r_j, s_{j+1})$ 
    Compute target  $y_j = r_j + \gamma \max_{a'} Q'(s_{j+1}, a'; \theta')$ 
    Perform gradient descent step on  $(y_j - Q(s_j, a_j; \theta))^2$ 
    if step mod target update frequency == 0 then
      Update target network:  $\theta' \leftarrow \theta$ 
    end if
    Update state  $s_t \leftarrow s_{t+1}$ 
  end for
end for

```

B. User study design

This IRB-approved study involved five healthy participants aged 22-36 years. The experimental setup included a Kinova Jaco robotic arm, an RGB camera for workspace perception, an Inertial Measurement Unit (IMU)-based head movement detector, and two randomly selected target objects which are supposed to be grasped by user inputs (see Fig. 4). The head movement detector measured the angle of the head toward the sides and decoded these movements into three discrete control inputs: right, left, and neutral. These user inputs was used to guide the robotic arm to reach two different target cups. A customized YOLOv8 [30] was trained for real-time object detection and distance tracking. The framework was generalized to handle a wide range of target objects including different types of cups, bottles, and containers. The reach-to-grasp operation in a planar 2D space required comparing Manual (pure head movement control) and Assistive (with STREAMS) modes. Each participant completed 40 trials: 20 in Manual mode and 20 in Assistive mode, with 10 trials for each target (left and right) in both modes. target positions remained constant throughout the experiment to have a systematic user study across participants. In this case study, users controlled lateral motion

through head movements, while the end-effector constantly moved 2 cm forward with each step. Only a noise level of 0.3 (p in 5) was added to simulate biosignal control for our user study. Grasping was automatically triggered whenever the end-effector was in proximity to the target sufficiently. Before data collection, participants were trained

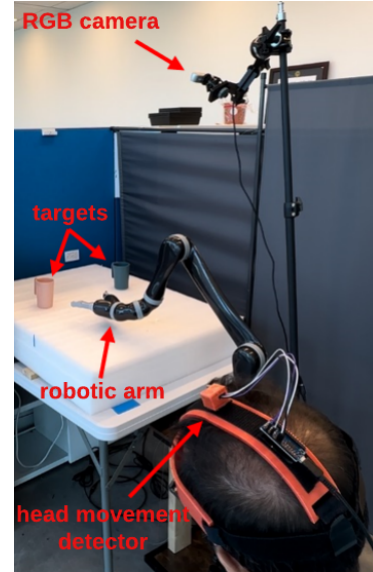


Fig. 4: Components of the STREAMS framework user study

in both modes and completed practice trials. Mode order was randomized to minimize learning effects. Data collection included video recording, trajectory extraction, targets and end-effector position tracking, and success rate recording. Participants also completed questionnaires on convenience, effort, and satisfaction for each mode. Performance metrics compared trajectory qualities, success rates, and user feedback between Manual and Assistive modes. A paired t-test was used to determine statistical significance of observed differences.

IV. RESULTS & DISCUSSION

A. Simulation

In Fig. 5, we investigated the performance of various reward functions designed to guide the robotic control system using the STREAMS framework. Three reward functions (R1, R2, and R3) were evaluated over 25,000 episodes, with R3 demonstrating better performance, reaching a peak average reward of 0.92. R1 and R2 also showed notable improvement, achieving maximum rewards of 0.71 and 0.73 respectively (Fig. 5a). All three functions exhibited an overall trend of improvement with increased training. In terms of efficiency, R3 achieved the quickest average grasping time at 11.90 steps, followed by R2 at 12.62 steps, and R1 at 13.54 steps (Fig. 5b). This shows that R3's time-penalized distance-based reward system was the most effective, while R2's distance-based rewards outperformed R1's binary reward system. The consistent learning curves across all three reward functions suggest that the STREAMS framework is robust and adaptable to different reward structures.

In Table I, we presented a comparison of success rates (SR) between manual and assistive modes across various noise levels and reward functions over 3000 test episodes. The results showed the assistive mode consistently outperformed the manual mode across all noise levels, with success rates above 91% even at the highest noise level. R3 achieved the best results, reaching 99.33% success under low noise (0.2) and maintaining 95.26% at high noise. STREAMS also demonstrated resilience to noise, with a minor performance drop compared to the sharper decline in manual mode, highlighting its robustness in noisy environments.

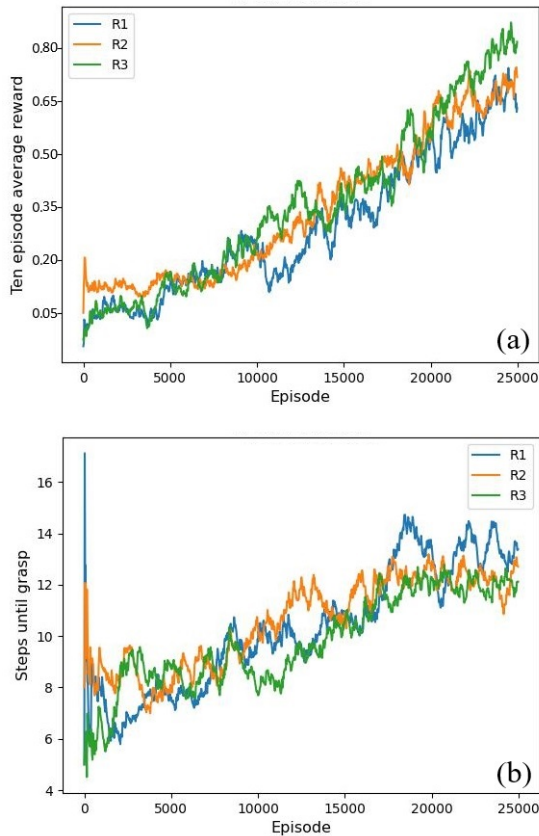


Fig. 5: Performance comparison of different reward functions (R1, R2, R3) in the STREAMS framework. (a) Ten-episode average reward over 25,000 episodes. (b) Number of steps required to grasp the target object per episode.

TABLE I: Success rates and standard deviations for manual and assistive modes at different noise levels.

Noise level	Manual mode SR (%)	Assistive mode SR (%)		
		R1	R2	R3
Low (0.2)	80.53 ± 2.34	98.53 ± 3.12	98.93 ± 1.87	99.33 ± 2.65
Medium (0.3)	74.26 ± 1.98	96.26 ± 4.11	97.83 ± 2.76	98.26 ± 3.44
High (0.4)	68.90 ± 3.75	91.26 ± 4.02	93.43 ± 2.49	95.26 ± 1.91

In Fig. 6, we illustrated the impact of noise on input signals and the resulting trajectories in both manual and assistive modes. Fig. 6(a) displays the input signals for low (purple), medium (green), and high (orange) noise levels. As the noise level increases, we can observe more frequent and erratic changes in the input signal. Fig. 6(b) and 6(c) show the traveled trajectories in a simulated environment.

Fig. 6(b) represents the manual mode, where the trajectories are visibly erratic and inefficient, particularly for the medium and high noise levels. These paths demonstrated significant deviation and unnecessary movements, reflecting the difficulty of precise control with direct noisy inputs. In contrast, Fig. 6(c) shows the trajectories generated by the STREAMS framework in assistive mode. The paths are noticeably smoother and more direct across all noise levels. Even with high noise, the STREAMS-assisted trajectory maintains a relatively straight path toward the target object. Fig. 6(d) shows a series of snapshots illustrating an example of a successful attempt where the robot arm moved toward the target object and grasped it.

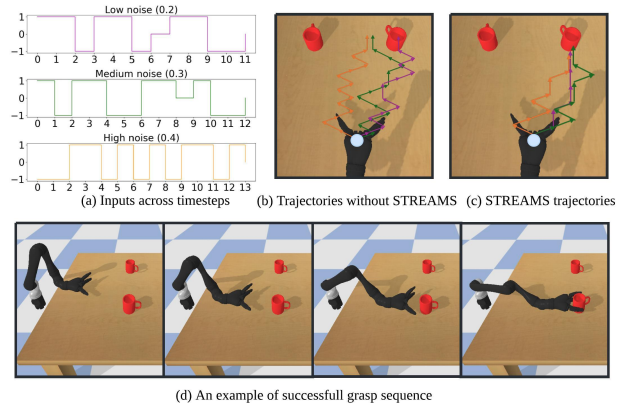


Fig. 6: Comparison of manual and STREAMS-assisted control under varying noise levels in the simulation environment. (a) Input signals. (b) Resulting trajectories in manual mode. (c) Improved trajectories using STREAMS in assistive mode. (d) Sequential snapshots of successful object grasping using STREAMS in a 3D environment.

B. User experiments

In Fig. 7, we compared user performance in manual mode versus assistive mode using the STREAMS framework across five subjects (S1-S5). We employed medium-level input noise (0.3) for head movements. The best-performing model from our simulation was adopted for the assistive mode. The visual data clearly illustrates the improvements in control and efficiency offered by the assistive mode. In manual mode, highly erratic and inefficient trajectories were observed for all subjects. The green (left target) and purple (right target) paths showed considerable deviation, and unnecessary movements, and often failed to reach the intended targets. This was reflected in low success rates ranging from 20% to 60%, with an average of just 44%. Conversely, the assistive mode displayed remarkably improved trajectories which consistently reached the intended targets. This improvement was quantified by substantially higher success rates, ranging from 75% to 90%, with an average of 83%. The p-value of <0.005 indicated that the outperformance in assistive mode is statistically significant.

The user study not only demonstrated quantitative improvements in performance but also revealed significant qualitative benefits of the STREAMS assistive mode. The

TABLE II: Summary of control methods and strategies in multimodal shared control assistive robotics.

Study	Approach	Modality	target-based	DoF	Dataset Req.	Accuracy
Jain et al. 2015 [20]	Sequential policies	IMU + Vision	Yes	6 (robot)	Yes	Not reported
Downey et al. 2016 [21]	Arbitrated policies	Spikes + Vision	No	4 (3D + grasp)	Yes	78%
Muelling et al. 2017 [22]	Arbitrated policies	Spikes + Vision	No	4 (3D + grasp)	Yes	73.74%
Xu et al. 2019 [23]	Arbitrated policies	EEG + Vision	Yes	2 (planar)	Yes	70%
Beraldo et al. 2022 [24]	Fused policies	EEG + Vision	No	2 (planar)	Yes	79.94%
Ours (STREAMS)	End-to-end self-learning policy	IMU* + Vision	No	3 (planar + grasp)	No	83%

* A generalizable approach for other signals as well, not limited to IMU input only.

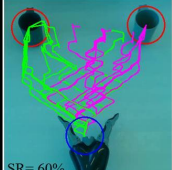
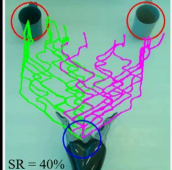
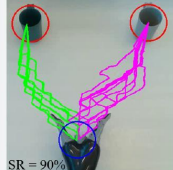
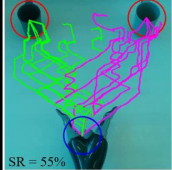
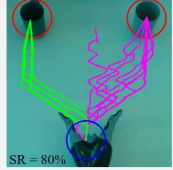
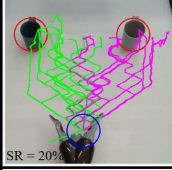
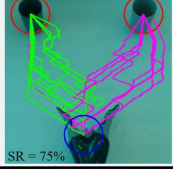
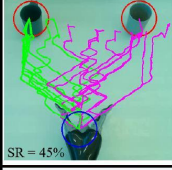
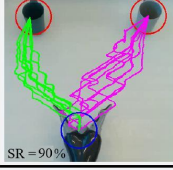
Subject	Manual mode	Assistive mode
S1	 SR = 60%	 SR = 80%
S2	 SR = 40%	 SR = 90%
S3	 SR = 55%	 SR = 80%
S4	 SR = 20%	 SR = 75%
S5	 SR = 45%	 SR = 90%
Avg SR	44%	83%
Std	15.57	6.71
p-value	<0.005	

Fig. 7: Comparison of manual and STREAMS-assisted control modes across five subjects (S1-S5). Each row shows trajectories for left (green) and right (purple) target objects, with success rates (SR). The bottom rows present average success rates, standard deviations, and statistical significance (p-value) of the performance difference between modes.

questionnaire included questions on task load (Q1) and overall satisfaction (Q2) for each mode, both rated on a

1-5 scale (1 = low, 5 = high). For Q1, the manual mode average score was 4.0, while the assistive mode score was 2.2. This substantial difference indicates that users found the task much less demanding when using the assistive mode. The lower cognitive load in assistive mode suggests that STREAMS effectively reduces the mental and physical effort required to complete the grasping tasks. For Q2, the manual mode average rate was 1.8, while the assistive mode rate was 4.0. Users clearly preferred the STREAMS-assisted control, likely due to the increased success rate and reduced effort required. These subjective measures align well with the objective performance data shown in Fig. 7.

In Table II, we presented a comparison of shared autonomy approaches in assistive robotics where STREAMS achieved the highest accuracy at 83% with a 3-DoF system. Unlike other methods, STREAMS requires no pre-existing datasets or predefined arbitrated policies and it is highly adaptable to new environments and dynamic targets. Additionally, its flexible input modality (IMU*) supports various input types, extending beyond IMU and vision. While STREAMS has fewer degrees of freedom compared to some earlier studies [20], its non-target-based approach provides more flexibility in dynamic environments where targets may not be clearly defined. Moreover, STREAMS generates smooth and reliable trajectories even in the face of environmental uncertainties, dynamic targets, ambiguous human intentions, and imprecise user inputs, making it robust and reliable for real-world assistive applications.

V. CONCLUSION

This study introduced STREAMS as a task support framework for shared autonomy in assistive robotics, addressing the challenge of generating robust trajectories from unreliable and noisy user inputs for precise robotic grasping. Our generalizable framework incorporates several key components, including an end-to-end self-learning policy for interaction with dynamic user intent and adaptation to environmental changes. STREAMS demonstrated the potential for generating smooth and stable trajectories across various noise levels and human users, without relying on pre-existing datasets. The efficacy of the proposed framework was validated in both simulated environments and real user cases, showing improvements in task performance and accuracy compared to manual control with no task support. Future research directions could include expanding the framework’s capabilities to handle more complex environments and tasks.

REFERENCES

- [1] A. Jackowski, M. Gebhard, and R. Thietje, "Head motion and head gesture-based robot control: A usability study," *IEEE Transactions on Neural Systems and Rehabilitation Engineering*, vol. 26, no. 1, pp. 161–170, 2017.
- [2] F. Rizzoglio, M. Giordano, F. A. Mussa-Ivaldi, and M. Casadio, "A non-linear body machine interface for controlling assistive robotic arms," *IEEE Transactions on Biomedical Engineering*, vol. 70, no. 7, pp. 2149–2159, 2023.
- [3] J. M. Lee, T. Gebrekristos, D. De Santis, M. Nejati-Javaremi, D. Gopinath, B. Parikh, F. A. Mussa-Ivaldi, and B. D. Argall, "Learning to control complex robots using high-dimensional body-machine interfaces," *ACM Transactions on Human-Robot Interaction*, 2024.
- [4] L. Wöhle and M. Gebhard, "Towards robust robot control in cartesian space using an infrastructureless head-and eye-gaze interface," *Sensors*, vol. 21, no. 5, p. 1798, 2021.
- [5] H. Admoni and S. Srinivasa, "Predicting user intent through eye gaze for shared autonomy," in *2016 AAAI fall symposium series*, 2016.
- [6] A. Rabiee, S. Ghafoori, A. Cetera, and R. Abiri, "Wavelet analysis of noninvasive eeg signals discriminates complex and natural grasp types," *arXiv preprint arXiv:2402.09447*, 2024.
- [7] R. Abiri, S. Borhani, E. W. Sellers, Y. Jiang, and X. Zhao, "A comprehensive review of eeg-based brain-computer interface paradigms," *Journal of neural engineering*, vol. 16, no. 1, p. 011001, 2019.
- [8] S. Ghafoori, A. Rabiee, A. Cetera, and R. Abiri, "Bispectrum analysis of noninvasive eeg signals discriminates complex and natural grasp types," *arXiv preprint arXiv:2402.01026*, 2024.
- [9] T. Teramae, T. Noda, and J. Morimoto, "Emg-based model predictive control for physical human-robot interaction: Application for assist-as-needed control," *IEEE Robotics and Automation Letters*, vol. 3, no. 1, pp. 210–217, 2017.
- [10] M. Ehrlich, Y. Zaidel, P. L. Weiss, A. Melamed Yekel, N. Gefen, L. Supic, and E. Ezra Tsur, "Adaptive control of a wheelchair mounted robotic arm with neuromorphically integrated velocity readings and online-learning," *Frontiers in Neuroscience*, vol. 16, p. 1007736, 2022.
- [11] R. Abiri, S. Borhani, J. Kilmarx, C. Esterwood, Y. Jiang, and X. Zhao, "A usability study of low-cost wireless brain-computer interface for cursor control using online linear model," *IEEE transactions on human-machine systems*, vol. 50, no. 4, pp. 287–297, 2020.
- [12] D. B. Silversmith, R. Abiri, N. F. Hardy, N. Natraj, A. Tu-Chan, E. F. Chang, and K. Ganguly, "Plug-and-play control of a brain-computer interface through neural map stabilization," *Nature biotechnology*, vol. 39, no. 3, pp. 326–335, 2021.
- [13] J. Kilmarx, R. Abiri, S. Borhani, Y. Jiang, and X. Zhao, "Sequence-based manipulation of robotic arm control in brain machine interface," *International Journal of Intelligent Robotics and Applications*, vol. 2, pp. 149–160, 2018.
- [14] A. Billard and D. Kragic, "Trends and challenges in robot manipulation," *Science*, vol. 364, no. 6446, p. eaat8414, 2019.
- [15] A. P. Dani, I. Salehi, G. Rotithor, D. Trombetta, and H. Ravichandrar, "Human-in-the-loop robot control for human-robot collaboration: Human intention estimation and safe trajectory tracking control for collaborative tasks," *IEEE Control Systems Magazine*, vol. 40, no. 6, pp. 29–56, 2020.
- [16] A. D. Dragan and S. S. Srinivasa, "A policy-blending formalism for shared control," *The International Journal of Robotics Research*, vol. 32, no. 7, pp. 790–805, 2013.
- [17] D. Gopinath, S. Jain, and B. D. Argall, "Human-in-the-loop optimization of shared autonomy in assistive robotics," *IEEE robotics and automation letters*, vol. 2, no. 1, pp. 247–254, 2016.
- [18] T. Carlson and Y. Demiris, "Collaborative control for a robotic wheelchair: evaluation of performance, attention, and workload," *IEEE Transactions on Systems, Man, and Cybernetics, Part B (Cybernetics)*, vol. 42, no. 3, pp. 876–888, 2012.
- [19] M. Gualtieri, J. Kuczynski, A. M. Shultz, A. Ten Pas, R. Platt, and H. Yanco, "Open world assistive grasping using laser selection," in *2017 IEEE International Conference on Robotics and Automation (ICRA)*. IEEE, 2017, pp. 4052–4057.
- [20] S. Jain, A. Farshchiansadegh, A. Broad, F. Abdollahi, F. Mussa-Ivaldi, and B. Argall, "Assistive robotic manipulation through shared autonomy and a body-machine interface," in *2015 IEEE international conference on rehabilitation robotics (ICORR)*. IEEE, 2015, pp. 526–531.
- [21] J. E. Downey, J. M. Weiss, K. Muelling, A. Venkatraman, J.-S. Valois, M. Hebert, J. A. Bagnell, A. B. Schwartz, and J. L. Collinger, "Blending of brain-machine interface and vision-guided autonomous robotics improves neuroprosthetic arm performance during grasping," *Journal of neuroengineering and rehabilitation*, vol. 13, pp. 1–12, 2016.
- [22] K. Muelling, A. Venkatraman, J.-S. Valois, J. E. Downey, J. Weiss, S. Javdani, M. Hebert, A. B. Schwartz, J. L. Collinger, and J. A. Bagnell, "Autonomy infused teleoperation with application to brain computer interface controlled manipulation," *Autonomous Robots*, vol. 41, pp. 1401–1422, 2017.
- [23] Y. Xu, C. Ding, X. Shu, K. Gui, Y. Bezudnova, X. Sheng, and D. Zhang, "Shared control of a robotic arm using non-invasive brain-computer interface and computer vision guidance," *Robotics and Autonomous Systems*, vol. 115, pp. 121–129, 2019.
- [24] G. Beraldo, L. Tonin, J. d. R. Millán, and E. Menegatti, "Shared intelligence for robot teleoperation via bmi," *IEEE Transactions on Human-Machine Systems*, vol. 52, no. 3, pp. 400–409, 2022.
- [25] M. C. Piastra, A. Nüßing, J. Vorwerk, M. Clerc, C. Engwer, and C. H. Wolters, "A comprehensive study on electroencephalography and magnetoencephalography sensitivity to cortical and subcortical sources," *Human Brain Mapping*, vol. 42, no. 4, pp. 978–992, 2021.
- [26] M. A. Rahman, F. Khanam, M. K. Hossain, M. K. Alam, and A. Mo-hiuddin, "Four-class motor imagery eeg signal classification using pca, wavelet and two-stage neural network," *International Journal of Advanced Computer Science and Applications*, vol. 10, no. 5, 2019.
- [27] X. Zhao, D. Liu, L. Ma, Q. Liu, K. Chen, S. Xie, and Q. Ai, "Deep cnn model based on serial-parallel structure optimization for four-class motor imagery eeg classification," *Biomedical Signal Processing and Control*, vol. 72, p. 103338, 2022.
- [28] Q. Ai, A. Chen, K. Chen, Q. Liu, T. Zhou, S. Xin, and Z. Ji, "Feature extraction of four-class motor imagery eeg signals based on functional brain network," *Journal of neural engineering*, vol. 16, no. 2, p. 026032, 2019.
- [29] S. Ge, R. Wang, and D. Yu, "Classification of four-class motor imagery employing single-channel electroencephalography," *PloS one*, vol. 9, no. 6, p. e98019, 2014.
- [30] G. Jocher, A. Chaurasia, and J. Qiu, "Ultralytics YOLO," Jan. 2023. [Online]. Available: <https://github.com/ultralytics/ultralytics>